Where $f_r$ is called rolling resistance coefficient.

The aerodynamic drag force $D_A$ can be expressed as:

$$D_A = \frac{1}{2}\rho v^2{}_{car} C_D A = \frac{1}{2}\rho(\dot{\theta}_{DM} r_{wh})^2 C_D A \qquad (2.3\text{-}17)$$

Where $\rho$ is air density, $r_{wh}$ is radius of wheels, and $v_{car}$ is speed of the car which equals to $\dot{\theta}_{DM} r_{wh}$ if the wind speed is zero, otherwise, it should be the relative speed between car and wind. $C_D$ is aerodynamic drag coefficient, which is determined empirically from car, and $A$ is frontal area of the car.

According to Eq.(2.3-13) where $T_{DM}$ is the torque that acts on wheels, Eq.(2.3-15) can be expressed as:

$$T_{DM} = I_{wh}\ddot{\theta}_{DM} + C_{wh}\dot{\theta}_{DM} + (M_{car}\ddot{\theta}_{DM} r_{wh} + R_x + D_A + R_{hx} + W_{car}\sin\theta_{load}) r_{wh} \qquad (2.3\text{-}18)$$

Where $I_{wh}$ is the identity inertia moment of the four wheels and $C_{wh}$ is the identity damping coefficient on wheels.

## 2.4 Dynamic Model Creation

Dynamic models according to system dynamic equations discussed in previous subsections are created into computer program in this section.

There are many commercial packages available to create dynamic models and do dynamic analysis, for example: Adams®, Working Model®, Visual Nastrain®, etc. However, the difficulty in engineering is not just the analyses of dynamic or static problems, but the problems to combine dynamic characters to control design, since the final purpose of engineering is to create a machine that is workable as expectation. Packets like Adams®, Working Model®, Visual Nastrain®, etc. are convenient for dynamic analysis. However, it is difficult to combine such dynamic characters to control design.

Engineering problems, whatever dynamic problem or control problem, are all sorts of math problems. The study here combines both dynamic problems, control problems, and optimization problems. The best way to solve all these problems integrally is to solve by mathematical methods which is the basis of all these engineering problems. Matlab®, a mathematically based engineering package produced by Math Work is used, because one of its packages: Simulink®, is able to create system equations with modules, which is one of the objectives in this study as mentioned in section 1.2 .

### 2.4.1 Matlab Simulink

Simulink® is one of the packages in Matlab®. In Simulink®, system equations can be created into a block according to the mechanical structure it belongs. And then with blocks created, many blocks can be combined into a grater block which can represent a complete system be simulated. Relations between block and block are connected by transfer lines defined in Simulink®. Each transfer line has one end of input and one or more ends of output that transfers parameters or variables it connects. And the combination of blocks can be in the form of close loop, where iterations are done automatically in the computing core.

In the following subsections, dynamic models of clutch actuator and AMT powertrain are created into Matlab® Simulink according to the system equations developed before

### 2.4.2 Module Creation

In this subsection, program models are created according to each component defined previously.

The components created here are combined further in subsection 2.4.4 .

### Electrical Motor

The system equations of the electrical motor are shown in Eq.(2.2-3) and Eq.(2.2-5). From Eq.(2.2-5), using Laplace Transform, current through armature can be obtained. According to the current, torque generated by electrical motor can be obtained from Eq.(2.2-3). The blocks according to these operations and equations in Simulink® are shown in Figure 2.4-1.

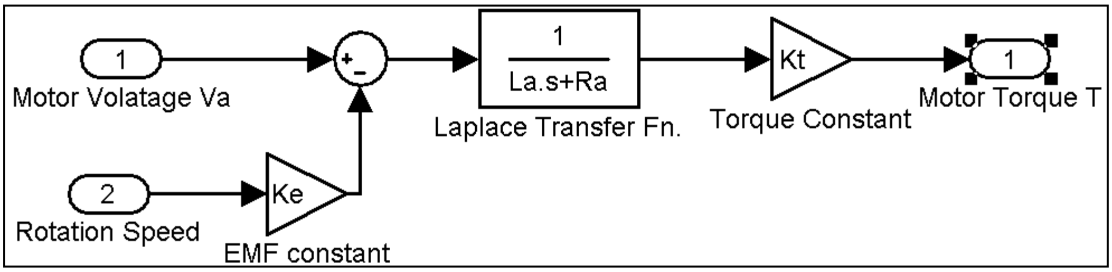


**Figure 2.4-1 Electrical Motor in Simulink® Model**

Combining these operating blocks, system dynamic equations of electrical motor can be created into an electrical motor module, as shown in Figure 2.4-2.

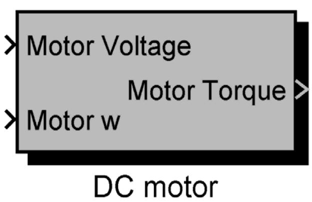


**Figure 2.4-2 DC Motor Module**

The parameters in this module are stated in Table 2.4-1.

| | |
|---|---|
| **Input** | $v_a$ , $\dot{\theta}_m$ |
| **Output** | $T$ |
| **System Parameters** | $K_t$ , $K_e$ , $La$ , $R_a$ |

**Table 2.4-1 Parameter Table of Electrical Motor**

### Worm Shaft

System equations of the worm shaft are shown in Eq.(2.2-12) and depends on Eq.(2.2-10) and Eq.(2.2-11). Creating the equations into Simulink®, the blocks are shown in Figure 2.4-3.

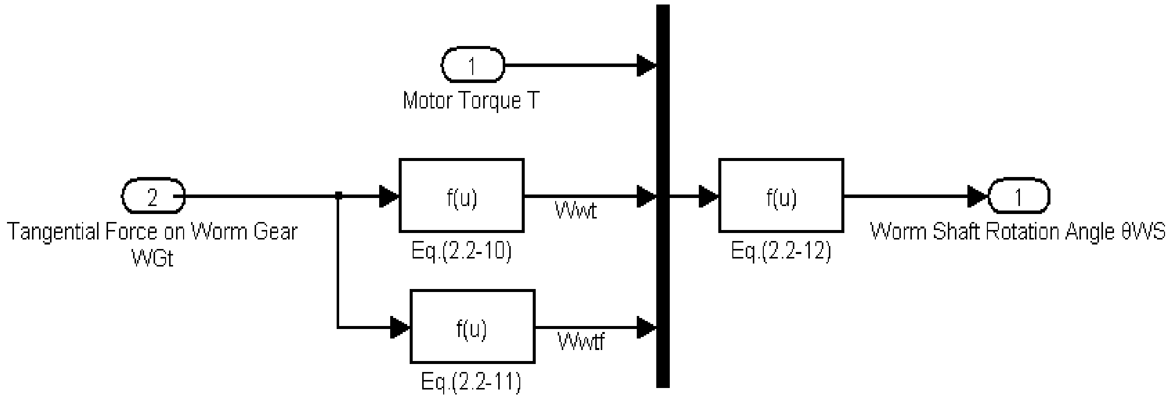


**Figure 2.4-3 Worm Shaft in Simulink® Model**

The parameters in this module are stated in Table 2.4-2.

| | |
|---|---|
| **Input** | $T$ , $W_{Gt}$ |
| **Output** | $\theta_{WS}$ |
| **System Parameters** | $I_{WS}$ , $C_{WS}$ , $\phi_n$ , $\lambda$ , $\mu$ , $d_W$ |

**Table 2.4-2 Parameter Table of Worm Shaft**

Note that equation blocks in figures above not completely state the equations developed before, but simplified diagrams which include many operators within the blocks used to solve the equations. In this study, for example, most of second order differential equations are solved by Laplace Transform method [21], transferring original equations to Laplace transfer functions for easier computing. For instance, electrical motor module stated above solving Eq.(2.2-3) and Eq.(2.2-5) using blocks in Figure 2.4-1 and finally merges these operating blocks to a combined module. On the other hand, system equations of each component, including many mathematical equations and operators as blocks, are combined into a bigger block as a module, as shown in Figure 2.4-2. Such process is reiterative in each component. Thus, the same process is not stated in the following discussions.

**Worm Gear**

System dynamic equation of worm gear is shown in Eq.(2.2-16), which is a general condition where the working angle is between upper an lower limits. A diagram of system equation created in Simulink® is shown in Figure 2.4-4

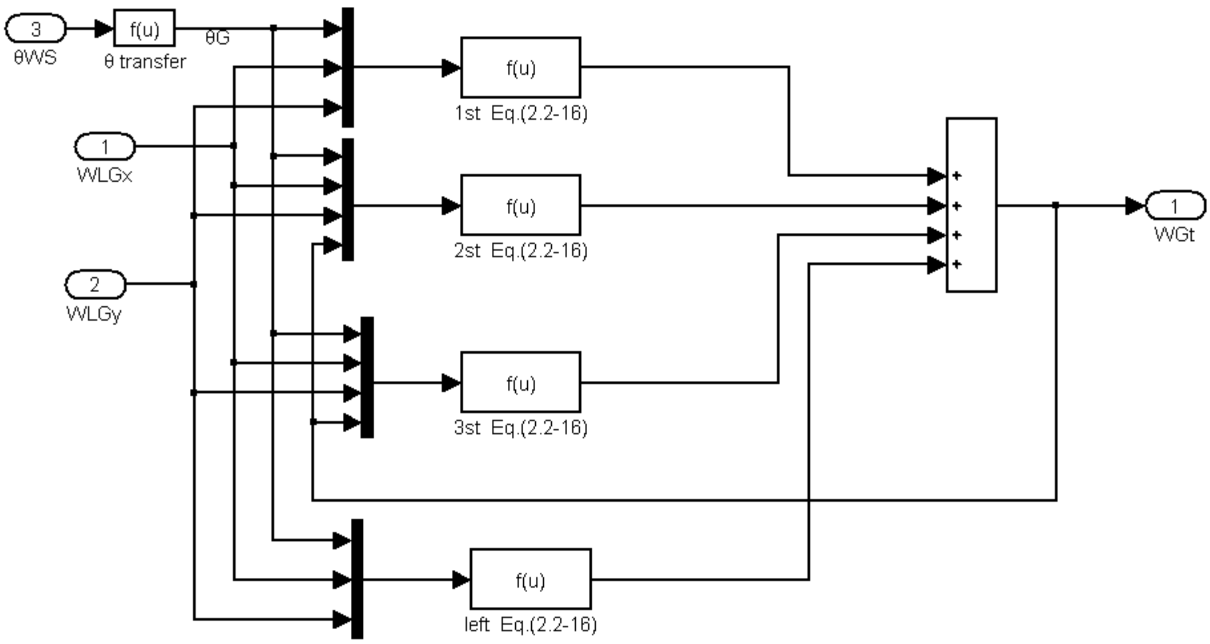


**Figure 2.4-4 Worm Gear in Simulink® Model**

Besides the general condition, the dynamic model should also consider the collision states as shown in Figure 2.2-12 and Figure 2.2-13. The system equations of such states are stated in Eq.(2.2-17). To check the condition, the model should estimate the rotation angle overtakes the upper/lower limits or not. If collision occurs, the model shown in Figure 2.4-4 should add a collision term as expressed in Eq.(2.2-17). Model of such condition is shown in Figure 2.4-5.

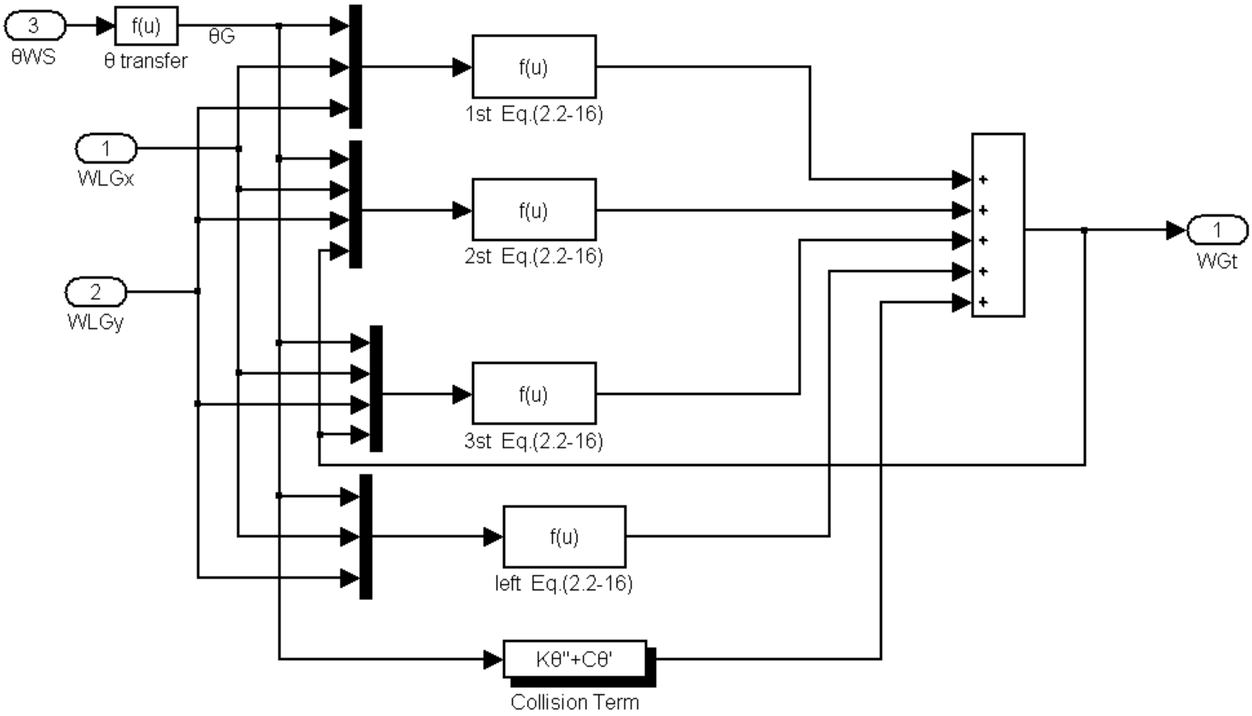


**Figure 2.4-5 Collision Model of Worm Gear**

The parameters in this model are shown in Table 2.4-3.

| | |
|---|---|
| **Input** | $\theta_{WS}$, $W_{LGx}$, $W_{LGy}$ |
| **Output** | $W_{Gt}$ |
| **System Parameters** | $I_G$, $C_G$, $R_G$, $r_G$, $\theta_{GL}$, $\phi_n$, $\lambda$, $\mu_{Ga}$, $\mu_{Gj}$, $R_{GP}$, $r_{GG}$, $m_G$, $R_{GJ}$, $K_c$, $C_c$ |

**Table 2.4-3 Parameter Table of Worm Gear**

### Linkage System

The system equations of linkage system are shown in Eqs.(2.2-23).

Besides Eqs.(2.2-23), Eq.(2.2-21), Eq.(2.2-22), and Eq.(2.2-24) provide some relations of inputs and outputs. From these equations, the dynamic model can be expressed in diagram as shown in Figure 2.4-6.

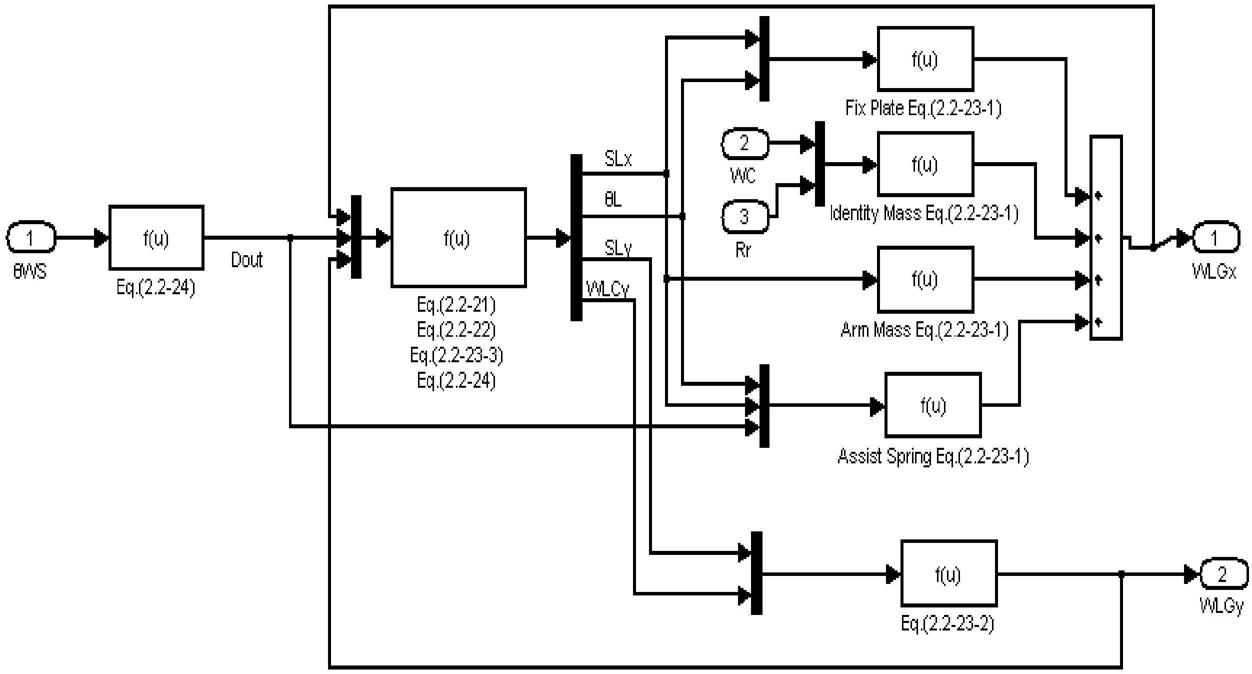


**Figure 2.4-6 Linkage System in Simulink® Model**

The parameters in this model are shown in Table 2.4-4.

| | |
|---|---|
| **Input** | $\theta_{WS}$, $W_c$, $R_r$ |
| **Output** | $W_{LGx}$, $W_{LGy}$ |
| **System Parameters** | $m_{BL}$, $C_{BL}$, $L_{Lb}$, $L_{La}$, $L_{LC}$, $m_L$, $M_{SP}$, $C_{SP}$, $K_{SP}$, $s_{ins}$, $\mu_{Gj}$, $\mu_{LC}$, $R_{GJ}$, $R_{LC}$ |

**Table 2.4-4 Parameter Table of Linkage System**

**Engine**

According to Table 2.3-1 and using interpolation-extrapolation method to compute the output torques where no experiment is available, the engine torque map according to engine speed and TPS in shown in Figure 2.3-4.

In Matlab® Simulink, such data can be computed using 2-D lookup table, which has two inputs: TPS and engine speed, and one output of engine torque. As shown in Figure 2.4-7.

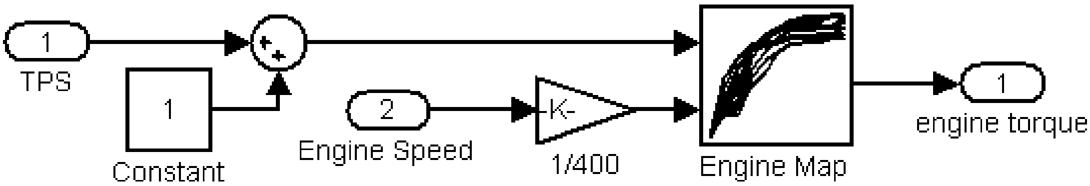


**Figure 2.4-7 Engine Map in Simulink® Model**

**Clutch**

System equation of the clutch is stated in Eq.(2.3-6). Besides, Eq.(2.3-3), Eq.(2.3-4), and Eq.(2.3-5) show the dynamic characters of the clutch.

The model of clutch system is complicated since it contains logical judgment, dynamic equations, and experiments data. Thus, the model creation chart here is not expressed with detail, where the complete system equations and logic judgment are expressed in 2.3.3 and the creation process is the same with above. Figure 2.4-8 just shows a diagram of simplified flowchart.

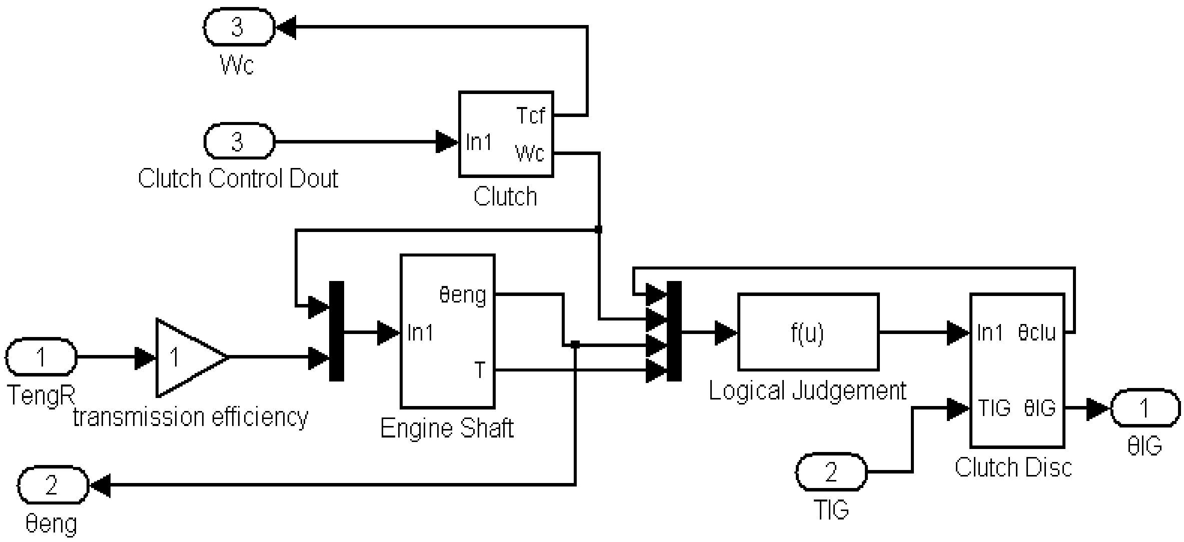


**Figure 2.4-8 Clutch in Simulink® Model**

The parameters in this model are stated in Table 2.4-5.

| | |
|---|---|
| **Input** | $T_{engR}$ , $D_{out}$ , $T_{IG}$ |
| **Output** | $\theta_{eng}$ , $W_c$ , $\theta_{IG}$ , |
| **System Parameters** | $I_{eng}$ , $C_{eng}$ , $\mu_{clutch}$ , $Ro$ , $Ri$ , $I_{CP}$ , $I_{ss}$ , $C_{CP}$ , $C_{ss}$ , $K_{ss}$ , $\eta_{eng}$ |

**Table 2.4-5 Parameter Table of Clutch**

**Gear Box**

The system equation of gear box in general condition is shown in Eq.(2.3-13). Combing with Eq.(2.3-12), an output of car speed can be obtained. The Simulink® model diagram is shown in Figure 2.4-9.

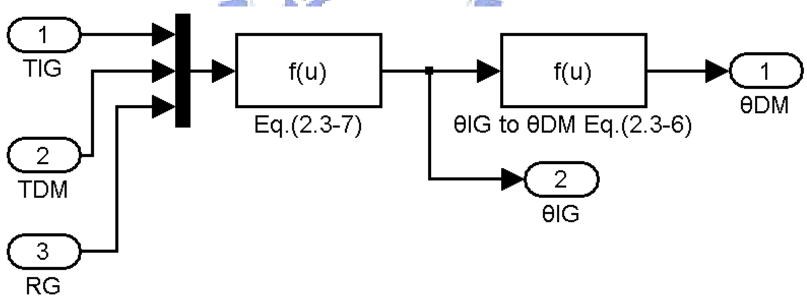


**Figure 2.4-9 Gear Box in Simulink® Model**

While shifting process is proceed, system equations should be transformed to Eqs.(2.3-14). The model built in Simulink® is shown in Figure 2.4-10.

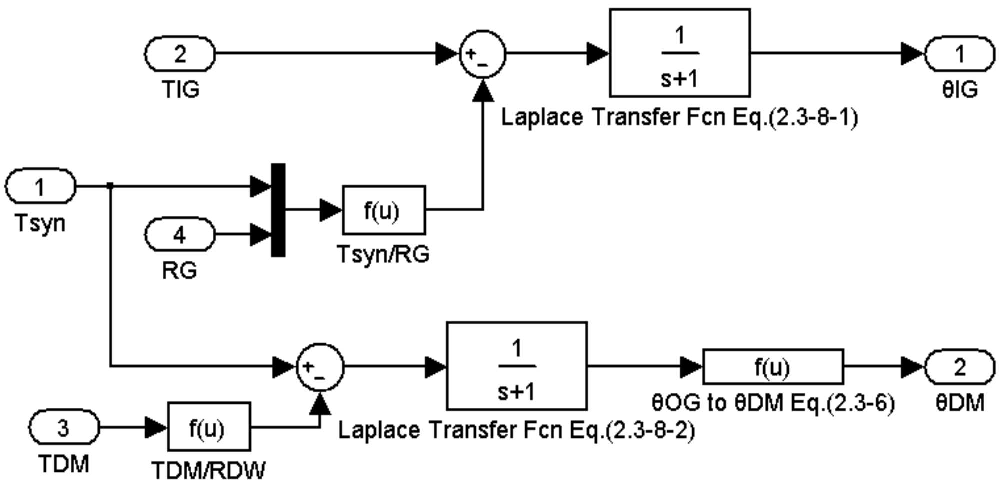


**Figure 2.4-10 Gear Box (Shifting) in Simulink® Model**

The parameters in this model are stated in Table 2.4-6.

| | |
|---|---|
| **Input** | $T_{IG}$, $T_{syn}$, $R_G$, $T_{DM}$ |
| **Output** | $\theta_{DM}$, $\theta_{IG}$ |
| **System Parameters** | $I_{IG}$, $I_{RG}$, $I_{OG}$, $I_{DM}$, $C_{IG}$, $C_{RG}$, $C_{OG}$, $C_{DM}$, $R_{DM}$, |

**Table 2.4-6 Parameter Table of Gear Box**

### Car Loading

The car loading equation is shown in Eq.(2.3-18). Figure 2.4-11 shows the diagram of this model.

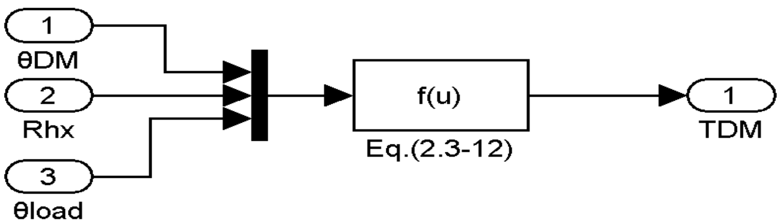


**Figure 2.4-11 Loading Function in Simulink® Model**

The parameters in this model are stated in Table 2.4-7.

| | |
|---|---|
| **Input** | $\theta_{DM}$, $R_{hx}$, $\theta_{load}$ |
| **Output** | $T_{DM}$ |
| **System Parameters** | $M_{car}$, $g$, $f_r$, $\rho$, $r_{wh}$, $C_D$, $A$, $I_{wh}$, $C_{wh}$ |

**Table 2.4-7 Parameter Table of Car Loading**

### 2.4.3 Parameter Setting

According to the models created in previous subsection, system parameters revealed in Table 2.4-1 to Table 2.4-7 are set here.

There are three methods to set the system parameters in this study: experiments data, table data, and CAD model computation. Most dimensions of components have been defined in the prototype; such parameters can be set directly from the design chart. Other properties of the components, like masses and inertia moments, are estimated by creating CAD model in Catia, and then computing inertia properties according to the materials applied. Parameters of some structures that are too complex to be built up into CAD model like engine, gear box, differential mechanism, etc., are determined by experiments data. Other parameters like friction coefficients, damping coefficients, air density, etc., are obtained by data tables.

Besides, note that static friction coefficients are set to be 1.2 times the dynamic friction coefficient in all models according to general conception [16].

Parameters of part dimension that have been defined in prototype design are shown in Table 2.4-8.

| $\phi_n$ | $\lambda$ | $d_W$ | $R_G$ | $\theta_{GL}$ | $R_{GP}$ | $R_{GJ}$ | $K_{SP}$ | $s_{ins}$ | $R_{LC}$ |
|---|---|---|---|---|---|---|---|---|---|
| $10.5^\circ$ | $5^\circ$ | 8mm | 34mm | $30^\circ$ | 3.5mm | 3mm | 0.6kg/mm | 40mm | 4mm |

| $M_{car}$ | $A$ | $R_{DM}$ | $r_{wh}$ | $R_G$ | $Ro$ |
|---|---|---|---|---|---|
| 1400kg | $2.74\,m^2$ | 5.375 | 0.287m | 3.945, 2.177, 1.394, 1.000, 0.853 | 95mm |

| $Ri$ | $R_r$ |
|---|---|
| 66mm | 1 |

**Table 2.4-8 Parameters from Prototype**

By CAD model created in Catia, parameters of some inertia moment and mass are obtained as shown in Table 2.4-9.

| $I_{WS}$ | $I_G$ | $m_G$ | $r_{GG}$ | $m_{BL}$ | $L_{La}$ | $L_{Lb}$ |
|---|---|---|---|---|---|---|
| 9.318e-7 $kg \cdot m^2$ | 9.861e-5 $kg \cdot m^2$ | 0.16kg | 12.8mm | 1.24kg | 60.748mm | 70.162mm |

| $L_{LC}$ | $m_L$ | $M_{SP}$ | $I_L$ |
|---|---|---|---|
| 44.762mm | 0.052kg | 0.048 | 9.828e-005 $kg \cdot m^2$ |

**Table 2.4-9 Parameters from Catia Models**

$M_{SP}$ is an identity mass of assist spring and fix plate, note that the mass of spring is not just the mass measured from CAD model.

In general, model of spring is simplified as Figure 2.4-12.

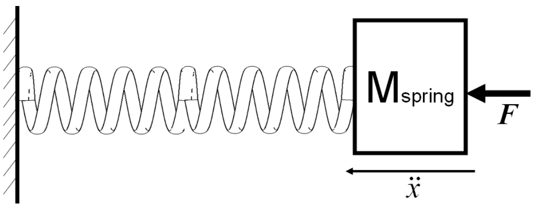


**Figure 2.4-12 General Spring Model**

However the mass of spring $M_{spring}$ in the general model can't just be the mass of spring from balance.

For an exact view of spring, a spring can be decomposed into many small masses, as shown in Figure 2.4-13.

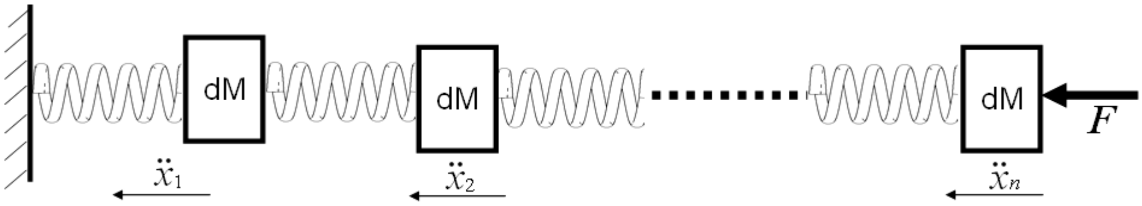


**Figure 2.4-13 Precise View of Spring Model**

From Figure 2.4-13, the system equation of spring, considering the term of mass $F_M$, can be expressed as:

$$F_M = \int_0^s (\frac{x}{s}\ddot{x}_{spring}\frac{m}{s})dx = \frac{m}{2}\ddot{x}_{spring} = M_{spring}\ddot{x}_{spring} \qquad (2.4\text{-}1)$$

Where each mass element $dM$ is expressed as $\frac{m}{s}dx$, and acceleration $\ddot{x}_n$ is expressed as $\frac{x}{s}\ddot{x}_{spring}$, where s is length of spring, $\ddot{x}_{spring}$ is longitudinal acceleration of spring at right end.

Thus, the mass of spring $M_{spring}$ is appointed to $\frac{m}{2}$, where $m$ is the mass of spring from balance.

Table 2.4-10 shows parameters obtained from experiments data.

| $I_{IG}$ | $I_{RG}$ | $I_{OG}$ | $I_{DM}$ | $C_{IG}$ | $C_{RG}$ |
|---|---|---|---|---|---|
| 0.074 $kg \cdot m^2$ | 1.4e-3 $kg \cdot m^2$ | 0.74e-3 $kg \cdot m^2$ | 2e-3 $kg \cdot m^2$ | 0.1 $N \cdot t/m$ | 0.01 $N \cdot t/m$ |

| $C_{OG}$ | $C_{DM}$ | $\mu_{clutch}$ | $\eta_{eng}$ | $C_{WS}$ | $C_G$ |
|---|---|---|---|---|---|
| 0.01 $N \cdot t/m$ | 0.05 $N \cdot t/m$ | 0.4 | 0.9 | 4.4e-6 $N \cdot t/m$ | 1e-6 $N \cdot t/m$ |

| $C_{BL}$ | $C_{SP}$ | $f_r$ | $C_D$ | $C_{wh}$ | $I_{eng}$ |
|---|---|---|---|---|---|
| 1e-9 $N \cdot t/m$ | 1e-7 $N \cdot t/m$ | 0.01386 | 0.53 | 0.1 $N \cdot t/m$ | 0.074 $kg \cdot m^2$ |

| $C_{eng}$ | $\mu_{clutch}$ | $I_{CP}$ | $I_{ss}$ | $C_{CP}$ | $K_{ss}$ |
|---|---|---|---|---|---|
| 0.15 $N \cdot t/m$ | 0.4 | 0.001 $kg \cdot m^2$ | 5e-3 $kg \cdot m^2$ | 1e-4 $N \cdot t/m$ | 735.47 $N \cdot m / arc$ |

| $C_{ss}$ | $T_{syn}$ |
|---|---|
| 0.1 $kg/t$ | 0.1 $N \cdot m$ |

**Table 2.4-10 Parameters from Experiments data**

Besides, torque constant $K_t$, EMF constant $K_e$, and armature resistance $R_s$ of electrical motor can be obtained from experiments data too. Table 2.4-11 shows experiment data of electrical motor of the clutch actuator.

| | | | | | | | |
|---|---|---|---|---|---|---|---|
| Torque | 3 | 3.15 | 4.19 | 5.1 | 5.61 | 6.18 | 7.42 |
| $\omega$ (R.P.M.) | 6788 | 6779 | 6738 | 6630 | 6469 | 6309 | 6174 |
| Current | 5.006 | 5.103 | 5.249 | 5.684 | 6.624 | 7.185 | 7.735 |
| Voltage | 12.11 | 12.1 | 12.07 | 12 | 11.94 | 11.88 | 11.85 |

| | | | | | | | |
|---|---|---|---|---|---|---|---|
| Torque | 8.22 | 9.42 | 10.12 | 10.97 | 11.92 | 12.8 | 13.8 |
| $\omega$ (R.P.M.) | 6059 | 5948 | 5831 | 5707 | 5586 | 5468 | 5350 |
| Current | 8.259 | 8.744 | 9.243 | 9.598 | 10.335 | 11.037 | 11.66 |
| Voltage | 11.82 | 11.79 | 11.75 | 11.69 | 11.66 | 11.61 | 11.57 |

| | | | | | | | |
|---|---|---|---|---|---|---|---|
| Torque | 14.45 | 15.32 | 16.12 | 17.12 | 18 | 18.72 | 19.52 |
| $\omega$ (R.P.M.) | 5229 | 5109 | 4989 | 4870 | 4751 | 4631 | 4511 |
| Current | 12.084 | 12.52 | 13.038 | 13.462 | 14.108 | 14.734 | 15.35 |
| Voltage | 11.54 | 11.49 | 11.44 | 11.39 | 11.34 | 11.31 | 11.25 |

| | | | | | | | |
|---|---|---|---|---|---|---|---|
| Torque | 20.4 | 21.12 | 22.27 | 23.67 | 24.17 | 25.12 | 26.2 |
| $\omega$ (R.P.M.) | 4392 | 4272 | 4155 | 4040 | 3917 | 3796 | 3678 |
| Current | 15.721 | 16.21 | 17.229 | 17.819 | 18.31 | 19.09 | 19.656 |
| Voltage | 11.2 | 11.15 | 11.11 | 11.1 | 11.08 | 11.04 | 10.99 |

| | | | | | | | |
|---|---|---|---|---|---|---|---|
| Torque | 27.2 | 27.57 | 28.47 | 29.27 | 30.6 | 30.7 | 31.87 |

| | | | | | | | |
|---|---|---|---|---|---|---|---|
| $\omega$(R.P.M.) | 3560 | 3436 | 3317 | 3201 | 3083 | 2959 | 2842 |
| Current | 20.117 | 20.137 | 21.037 | 21.946 | 22.52 | 23.086 | 23.519 |
| Voltage | 10.93 | 10.89 | 10.87 | 10.83 | 10.79 | 10.75 | 10.69 |

| | | | |
|---|---|---|---|
| Torque | 32.52 | 33.67 | 34.6 |
| $\omega$(R.P.M.) | 2724 | 2606 | 2487 |
| Current | 23.805 | 24.286 | 25.24 |
| Voltage | 10.63 | 10.58 | 10.54 |

**Table 2.4-11 Experiments Data of Electrical Motor**

From Eq.(2.2-3), which is the system equation of the electrical motor in terms of current and torque, using curve fitting method, the fitted curve is shown in Figure 1.1-1.

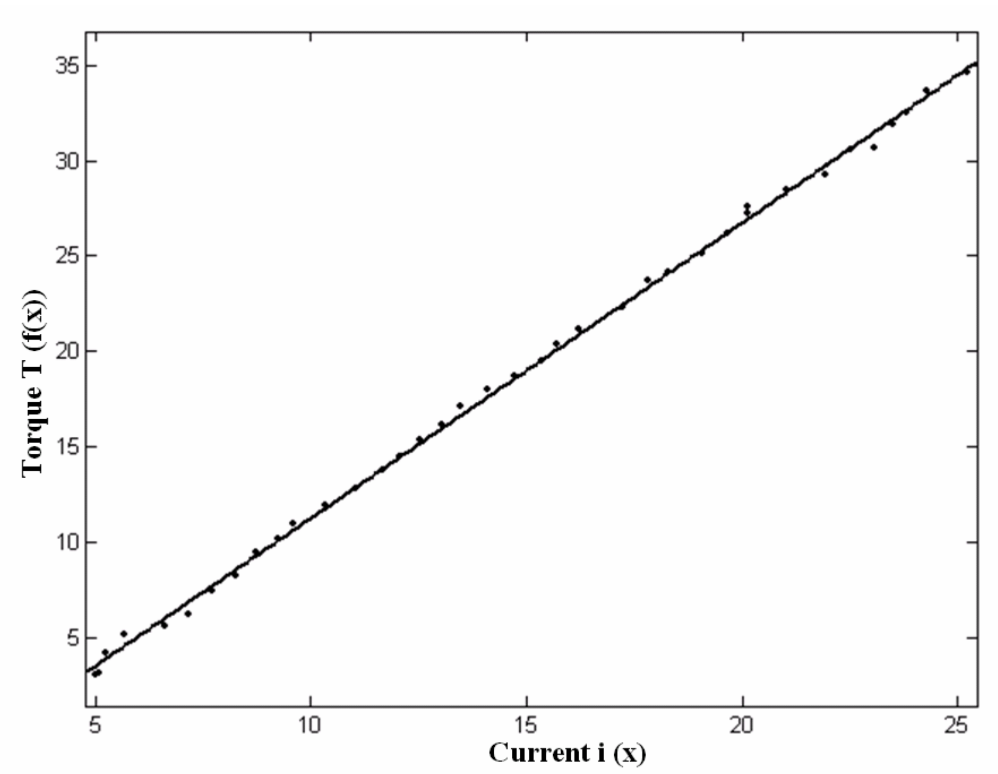


**Figure 2.4-14 Torque-Current Fitting Curve**

Where the fitted function is:

$$f(x) = 1.551x - 4.272 \tag{2.4-2}$$

Comparing to Eq.(2.2-3) $T = K_t i$, where $i$ corresponds to independent variable $x$, $T$ corresponds to function $f(x)$, $K_t$ is obtained as 1.551. The last term in Eq.(2.4-2) is a negative constant, which physically means that the torque is produced only after current $i$ arrives at a constant of $\frac{1.551}{4.272}$. This may be caused by capacitance which can lead to experiment error of current measure. However, the error doesn't influence the linear relation between current and torque, and the magnitude is small which can be ignored in the system equation.

Eq.(2.2-5) shows the relation between inductance, resistance, source voltage , and EMF constant. Since inductance is always small enough to be ignored [11], Eq.(2.2-5) can be expressed in matrix form as shown in Eq.(2.4-3)

$$\begin{bmatrix} i_a & \dot{\theta}_m \end{bmatrix} \begin{bmatrix} R_s \\ K_e \end{bmatrix} = v_a \tag{2.4-3}$$

Putting experiments data Table 2.4-11 into Eq.(2.4-3), the matrix form is shown below. Where n is the number of experiments according to different currents.

$$\begin{bmatrix} i_{a1} & \dot{\theta}_{m1} \\ i_{a2} & \dot{\theta}_{m2} \\ \vdots & \vdots \\ i_{a(n-1)} & \dot{\theta}_{m(n-1)} \\ i_{an} & \dot{\theta}_{mn} \end{bmatrix} \begin{bmatrix} R_s \\ K_e \end{bmatrix} = \begin{bmatrix} v_{a1} \\ v_{a2} \\ \vdots \\ v_{a(n-1)} \\ v_{an} \end{bmatrix} \tag{2.4-4}$$

The objective here is to solve $R_s$ and $K_e$ that best mesh to the experiments data: $i_{an}$, $\dot{\theta}_{mn}$, and $v_{an}$, which is a two unknowns with n equations algebraic problem.

To get the most approximate solution of $R_s$ and $K_e$ in Eq.(2.4-4), using least square error method, Eq.(2.4-4) can be solved using Eq.(2.4-5) [12].

$$\begin{bmatrix} i_{a1} & i_{a2} & \cdots & i_{a(n-1)} & i_{an} \\ \dot{\theta}_{m1} & \dot{\theta}_{m2} & \cdots & \dot{\theta}_{m(n-1)} & \dot{\theta}_{mn} \end{bmatrix} \begin{bmatrix} i_{a1} & \dot{\theta}_{m1} \\ i_{a2} & \dot{\theta}_{m2} \\ \vdots & \vdots \\ i_{a(n-1)} & \dot{\theta}_{m(n-1)} \\ i_{an} & \dot{\theta}_{mn} \end{bmatrix} \begin{bmatrix} R_s \\ K_e \end{bmatrix} = \begin{bmatrix} i_{a1} & i_{a2} & \cdots & i_{a(n-1)} & i_{an} \\ \dot{\theta}_{m1} & \dot{\theta}_{m2} & \cdots & \dot{\theta}_{m(n-1)} & \dot{\theta}_{mn} \end{bmatrix} \begin{bmatrix} v_{a1} \\ v_{a2} \\ \vdots \\ v_{a(n-1)} \\ v_{an} \end{bmatrix}$$

( 2.4-5)

Solving Eq.(2.4-5), $R_s = 0.2638$ and $K_e = 0.0016$ is obtained. A comparison of experiments data and least square error result is shown in Figure 2.4-15, where the dash line stands for experiments data.

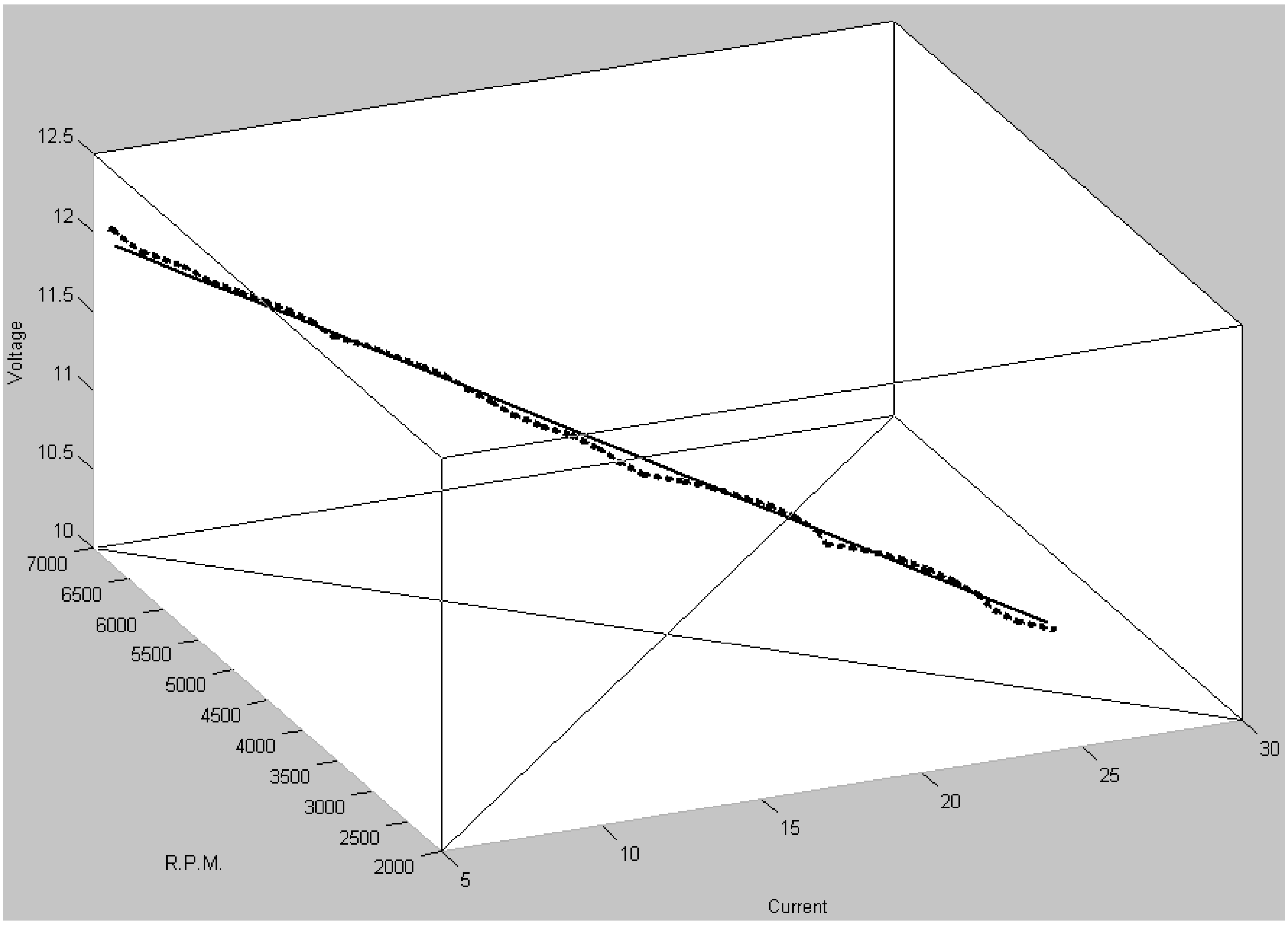


**Figure 2.4-15 Voltage-Current-Speed**

Table 2.4-12 shows other parameters obtained from tables [22] [23].

| $\mu$ | $\mu_{Ga}$ | $\mu_{GJ}$ | $K_c$ | $\mu_{LC}$ | $\rho$ |
|---|---|---|---|---|---|
| 0.26 | 0.33 | 0.2 | 3500kg/mm | 0.1 | $1.23\,kg/m^3$ |

**Table 2.4-12 Parameters from Tables**

### 2.4.4 Module Combination

Combining both input and output of modules created before, a system model of AMT transmission system is obtained, which mainly includes modules of clutch controller, DC motor, clutch actuator, clutch, engine, and powertrain, where the "Controller" module is defined in CHAPTER 3 and the "Powertrain" module includes gear box, differential gear, and vehicle loading. The combined system model is shown in Figure 2.4-16, where.

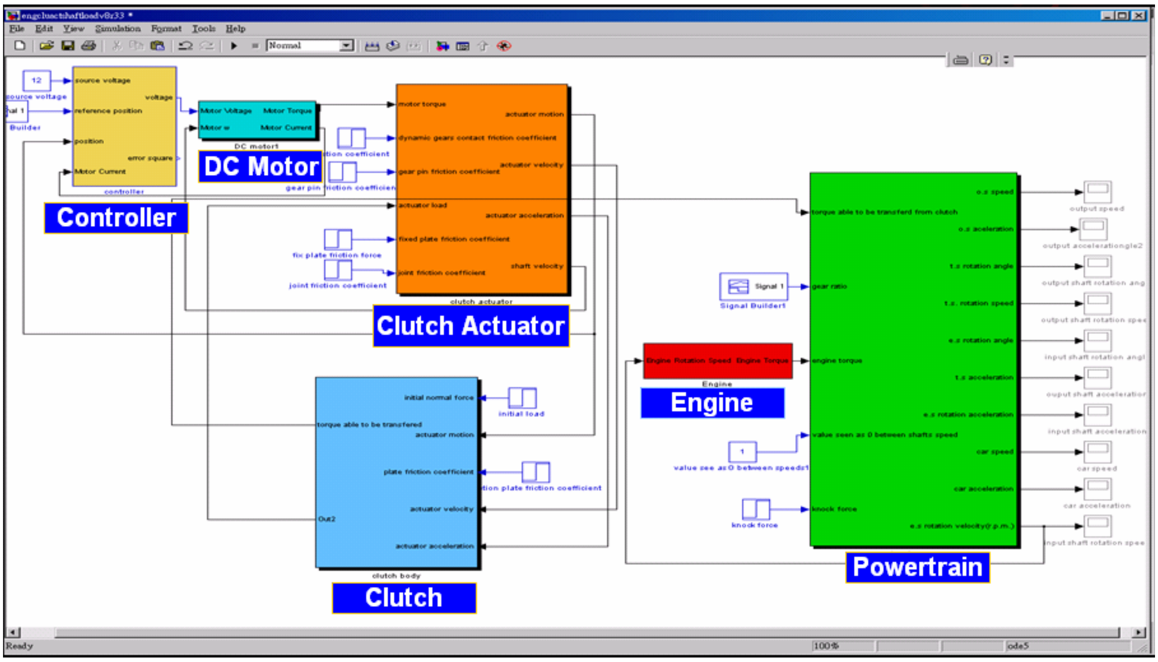


**Figure 2.4-16 Combined AMT System Model**

The main concept of module combination can be decomposed into two procedures. The first is motion transform, which introduces relative motions of each component according to the mechanism connecting. The second procedure computes loading of the each mechanical part from system equations, with accordance of forces exerted by other components caused by relative motions obtained from the first procedure. And the computed loadings of procedure two are transformed to motion by system equations than serve as the input of procedure one. A flowchart of such concept is shown in Figure 2.4-17.

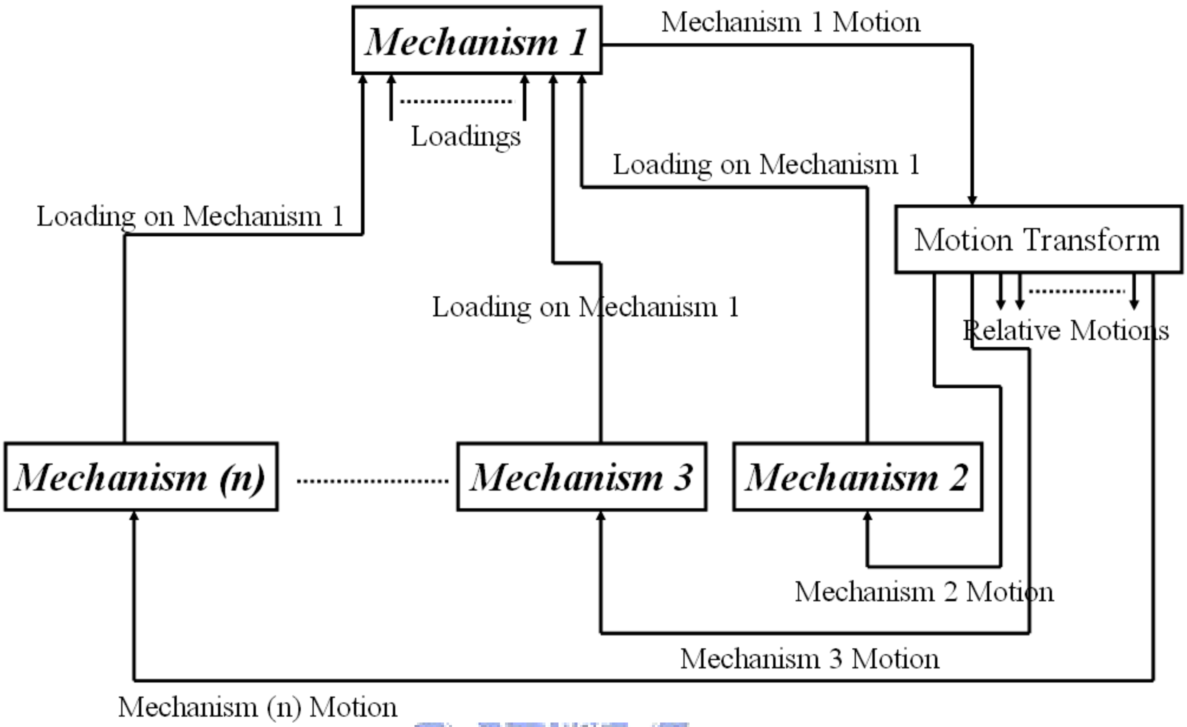


**Figure 2.4-17 Flowchart of Modules Combination**